Annular gap solitons in Kerr media with circular gratings

Jacob Scheuer[1,2] and Boris Malomed[1]
[1]*School of Electrical Engineering, Tel-Aviv University, Tel Aviv 69978, Israel*
[2]*The Center for Nanoscience and Nanotechnology, Tel-Aviv University, Tel Aviv 69978, Israel*
(Received 18 February 2007; published 6 June 2007)

We introduce standing-light patterns trapped in a Bragg grating written along the radial direction in a self-focusing (SF) or self-defocusing (SDF) optical medium. Unlike previously studied axisymmetric settings that deal with the axial propagation, we consider the propagation of light in the radial directions (outward and inward), which may give rise to *annular gap solitons* (AGSs), supported by the circular grating. An estimate for the threshold of the modulational instability of the AGS against azimuthal perturbations in the SF medium is obtained analytically, and verified by direct simulations. In the SDF model, stable annular and dipole solitons are found in a numerical form, while multipole patterns and vortex rings are unstable. Similar solitons are possible in the Bose-Einstein condensate.

DOI: 10.1103/PhysRevA.75.063805 PACS number(s): 42.65.Tg, 42.65.Jx, 42.79.Dj

I. INTRODUCTION

The propagation of electromagnetic waves in natural and artificially fabricated inhomogeneous nonlinear media exhibit a wide variety of phenomena, especially the formation of localized patterns [1], such as continuous and discrete solitons and vortices. A great deal of attention was also drawn to interactions between the solitons, beam steering [2], etc. The ability to control the transmission dynamics in spatially modulated media is crucially important for applications to optical telecommunications and data processing, manipulations of Bose-Einstein condensates (BECs) [3], and for other purposes.

Fundamental and vortical solitons have been predicted and created in materials combining the periodic modulation and Kerr or saturable nonlinearity (most of these materials belong to a broad class of *artificial optical media*, which actually constitute a central subject of experimental and theoretical studies in modern-day linear and nonlinear optics). In particular, discrete one-dimensional (1D) solitons, predicted in Ref. [4], were demonstrated in Ref. [5], which was followed by the creation of their 2D counterparts, supported by a photonic lattice in a photorefractive medium [6]. Vortex lattice solitons, which were predicted in Ref. [7], were created using a similar technique [8]. The photorefractive [9] and semiconductor-laser media [10] were also used to demonstrate the formation of regular arrays and necklace-shaped multisoliton patterns. Axisymmetric 2D solitons, including vortical ones, were predicted in radial lattices [11]. Recently, they were created using a photonic radial lattice in a photorefractive medium [12]. A recent result is the demonstration of the Anderson localization in a disordered array of waveguides induced in a photorefractive crystal by properly arranged laser illumination [13].

These studies were focused on *beams*, i.e., waves that are transversely self-trapped in two dimensions and propagate in the third direction. Here, we introduce a distinct type of "frozen" (standing) optical solitons created by light propagating in the *radial directions* in the 2D geometry. In the third dimension, the electromagnetic wave is confined by the slab configuration of the waveguide, while in the guiding plane it is made standing, in the form of a *light ring*, by a circular Bragg grating (CBG) [a necessary coherent source of light may be provided by a vertical cavity surface emitting laser (VCSEL) rod inserted at the pivot of the disk-shaped slab]. A schematic of a fabricated waveguide capable of hosting such optical patterns is shown in Fig. 1 [14]. The refractive-index profile in the dielectric slab corresponding to the CBG [its most efficient profile has the form given by Eq. (3), see below] can be fabricated by means of radial perforations (a somewhat similar structure is featured by the cross section of a hollow-core multilayer fiber [15]; however, it supports axial, rather than radial, light propagation).

An alternative experimental realization of the medium is possible in a slab waveguide made of a material with strong Kerr nonlinearity (such as AlGaAs), in which a *virtual* radial lattice can be induced by a transverse (cylindrical) strong laser beam, illuminating the slab in the axial direction. The radial intensity of the beam may be patterned as required [in particular, fitted to the profile given by Eq. (3)] by passing it through a properly designed mask. As mentioned above, a similar technique, which makes it possible to create radial photonic lattices of a required profile, was recently developed in photorefractive media [12]. Because the polarizations of the lattice-forming (pump) axial (cylindrical) beam and probe signal propagating along the radius (ρ) are orthogonal, their intensities simply sum up, $I_{\text{total}}=I_{\text{pump}}(\rho)+I_{\text{probe}}$, the first term inducing, through the Kerr effect, the necessary radial profile acting on the probe beam.

The paper is organized as follows. In Sec. II we introduce the CBG model and report approximate analytical results for annular solitons found in it. Various numerical results, which focus on the stability of annular, dipole, multipole, and vor-

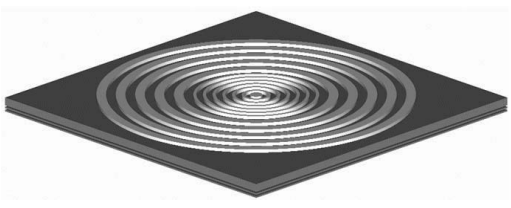

FIG. 1. A schematic of the circular Bragg grating.

tex solitons, are presented in Sec. III. The paper is concluded by Sec. IV.

II. THEORETICAL MODEL AND STABILITY ANALYSIS

The evolution of the amplitude of the electromagnetic field propagating in the CBG from the center outward, or reflected inward, obeys the wave equation

$$\rho^2 E_{\rho\rho} + \rho E_\rho + E_{\theta\theta} - (n/c_0)^2 \rho^2 E_{tt} = 0, \tag{1}$$

where ρ and θ are polar coordinates, c_0 is the speed of light in vacuum, and $n^2 = n_0^2 + 2n_0 n_2 |E|^2 + \Delta\varepsilon(\rho,\theta)$ is the total dielectric permittivity, with n_0 and n_2 the linear refractive index and Kerr coefficient, and $\Delta\varepsilon(\rho,\theta)/(2n_0)$ the local change of the refractive index which creates the CBG. In the framework of the coupled-mode theory, we approximate the solution by a superposition of inward and outward radial waves, with amplitudes U and V:

$$E = [U(\rho,\theta,t) H_m^{(1)}(k\rho) + V(\rho,\theta,t) H_m^{(2)}(k\rho)] \exp(-i\omega t), \tag{2}$$

where $k = n_0\omega/c$, ω is a common carrier frequency of the two waves, and $H_m^{(1,2)}$ are the Hankel functions of the first and second kind that represent the outward and inward waves in the linear approximation (integer m will be the angular propagation constant, alias *vorticity* of the solution, see below).

As shown in previous work [14], the profile of the refraction-index modulation providing for the most efficient linear coupling between the two radial waves via the resonant Bragg reflection is given by

$$\Delta\varepsilon(\rho) = \beta H_m^{(1)}(k\rho)/H_m^{(2)}(k\rho) + \text{c.c.}, \tag{3}$$

where $\beta \equiv \alpha \exp(i\varphi)$ is a (complex) coupling strength generated by this profile, and c.c. stands for complex conjugate. Inserting this profile and ansatz (2) into Eq. (1) and making use of rescalings, $\xi \equiv (\alpha\omega/2n_0 c)\rho$, $\eta \equiv (\alpha\omega/2n_0)t$, $\{u,v\} \equiv 2|H_m^{(1)}(\xi)|\sqrt{n_0 n_2/\alpha}\{\exp(-\frac{1}{2}i\varphi)U, \exp(+\frac{1}{2}i\varphi)V\}$, we arrive at a system of coupled-mode equations,

$$iu_\eta + iu_\xi + \frac{\alpha}{2\xi^2}(m^2 u + u_{\theta\theta}) + \sigma\left(\frac{1}{2}|u|^2 + |v|^2\right)v + v = 0,$$

$$iv_\eta - iv_\xi + \frac{\alpha}{2\xi^2}(m^2 v + v_{\theta\theta}) + \sigma\left(\frac{1}{2}|v|^2 + |u|^2\right)u + u = 0, \tag{4}$$

where $\sigma \equiv \text{sgn}(n_2) = +1$ and -1 for the self-focusing (SF) and self-defocusing (SDF) medium, respectively. The derivation of the coupled-mode equations implies that the characteristic (radial) size of the corresponding solitons is ~ 1000 periods of the grating, i.e., ~ 1 mm [16]. In such a case, gap solitons can be created in the real experiment (the creation of essentially narrower solitons may require the light intensity above the destruction threshold of glass) [16].

Following the pattern of exact gap-soliton solutions in the 1D model of nonlinear fiber Bragg gratings [17], we find solutions to Eq. (4) that represent *annular gap solitons* (AGSs). For $\sigma = +1$ (the SF model), these are

$$u = \sqrt{2/3}(\sin Q)\,\text{sech}\left(\xi \sin Q - \frac{i}{2}Q\right) e^{im\theta - i\eta\cos Q},$$

$$v = -\sqrt{2/3}(\sin Q)\,\text{sech}\left(\xi \sin Q + \frac{i}{2}Q\right) e^{im\theta - i\eta\cos Q}, \tag{5}$$

with a free parameter, Q, taking values $0 < Q < \pi$. In the SDF model ($\sigma = -1$), the solution is obtained from Eqs. (5) by the transformation $u \to u^*$, $v \to -v^*$.

Proceeding to the analysis of stability of the AGS, we notice that the 1D stability of solutions (5) is provided by condition $Q \geq C$ $(\pi/2)$, with $C \approx 1.01$ [18]. In fact, the case of Q essentially smaller than $\pi/2$ is most relevant to the experiment, the shape of the corresponding soliton being close to that in the nonlinear Schrödinger (NLS) equation [19].

A new issue, which makes the present model essentially different from its 1D counterpart, is stability of the ring-shaped solitons to *transverse* (azimuthal) perturbations. To derive an analytical approximation for the corresponding stability condition, we replace coefficient $1/\xi^2$ in Eqs. (4) by $1/\xi_0^2$, where ξ_0 is the average radius of the ring. In this approximation, long-wave transverse perturbations obey a simplified version of Eqs. (4),

$$iU_\eta + \frac{1}{2}U_{yy} + \sigma\left(\frac{1}{2}|U|^2 + |V|^2\right)U + V = 0,$$

$$iV_\eta + \frac{1}{2}V_{yy} + \sigma\left(\frac{1}{2}|V|^2 + |U|^2\right)V + U = 0, \tag{6}$$

where $y \equiv (\xi_0/\sqrt{\alpha})\theta$, and $\{U,V\} \equiv \{u,v\}\exp(-i\alpha m^2 \eta/2\xi_0^2)$. The condition of the 2π-periodicity in θ selects a discrete set of possible values of the y-wave number, $k_y = (\sqrt{\alpha}/\xi_0)l$, with $l = 0,1,2,\ldots$. AGS with amplitude A_0 corresponds to plane-wave solutions of Eqs. (6), $U = -V = A_0 \exp\{i[(3\sigma A_0^2/2) - 1]\}$.

To explore the azimuthal stability of the AGS, the respective infinitesimal perturbations are introduced as follows:

$$\begin{pmatrix} U \\ V \end{pmatrix} = \begin{pmatrix} A_0 + \gamma(\eta,y)e^{i\phi(\eta,y)} \\ -A_0 + \beta(\eta,y)e^{i\psi(\eta,y)} \end{pmatrix} \exp\{-i[(3\sigma/2)A_0^2 - 1]\eta\}, \tag{7}$$

where amplitude and phase perturbations are $(\gamma,\beta,\phi,\psi) = (\gamma_0,\beta_0,\phi_0,\psi_0)\exp(\delta\eta + ipy)$, with p a real perturbation wave number, which is subject to the same quantization condition as above,

$$p = (\sqrt{\alpha}/\xi_0)n, \quad n = 0,1,2,\ldots, \tag{8}$$

and δ the corresponding instability growth rate. The substitution of expressions (7) in Eqs. (6) and linearization lead to a dispersion equation which determines δ as a function of p for long-wave perturbations (i.e., small p and δ),

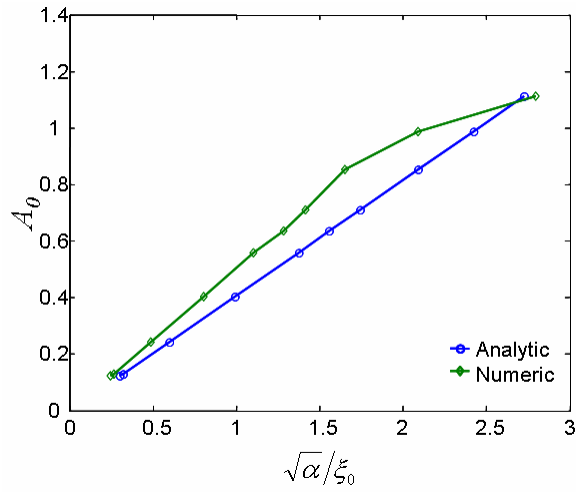

FIG. 2. (Color online) Comparison between the approximate analytical prediction for the stability border in the self-focusing model (with $\sigma=+1$), Eq. (10) (the straight line), and a numerically found stability border (rhombuses). The simulations were conducted using initial wave form (5), with $Q=0.5$ and $\xi_0=80$.

$$\delta^2 \approx (1/4)p^2(6\sigma A_0{}^2 - p^2), \tag{9}$$

where we assume that, as said above, in experimentally relevant settings A_0^2 is relatively small too, corresponding to the quasi-NLS soliton.

Equation (9) yields $\delta^2 \approx (3/2)\sigma A_0^2 p^2$ in the limit of $p^2 \to 0$, which means that the annular soliton is *transversely stable* (δ is imaginary) in the SDF model, with $\sigma=-1$. On the contrary to that, rectilinear solitons are always unstable against long-wave transverse perturbations in the SF medium, with $\sigma=1$. However, the quantization condition for the azimuthal perturbations around the annular soliton, given by Eq. (8), implies that the smallest allowed perturbation wave number, $p_{\min}^2=|\alpha|/\xi_0^2$, exceeds the instability cutoff in Eq. (9), $p_{\text{cutoff}}^2=6A_0^2$, if the mean radius and amplitude of the AGS satisfy the condition

$$6(\xi_0 A_0)^2 < \alpha. \tag{10}$$

Thus the curvature may stabilize the AGS in the SF medium, and the annular solitons in the SDF medium should definitely be stable. If the soliton's amplitude is taken as per solution (5), $A_0=2\sqrt{2/3}\sin(Q/2)$, condition (10) implies, after undoing the normalizations, that the stabilization is possible when the radius of the soliton ring is approximately equal to its width in the radial direction, bringing the situation to the brink of the parameter range in which the above derivation is valid. Therefore the analytical results may only be approximately correct, and the possibility of the stabilization of the annular solitons should be checked in direct simulations of Eqs. (4).

III. NUMERICAL SIMULATIONS

In simulations, the initial configuration was taken as radial soliton (5) with a perturbation imposed upon it in the form of a small sinusoidal modulation in the angular coordinate. Figure 2 displays a comparison between the approximate analytical prediction for the stability border, Eq. (10), and a numerically found stability limit. The proximity of the prediction to the numerical findings demonstrates that, if amplitude A_0 is not formally related to the soliton's width as per solution (5) (which, as a matter of fact, was not implied in the derivation of the criterion), then stability criterion (10) *correctly predicts* the stabilization of the AGS by the relatively small curvature (as Figs. 4 and 5 show below, at least up to the ratio ~40–50 of the average radius of the soliton ring to its radial width). The fact that the numerical analysis yields a slightly larger stability region than predicted analytically is explained by the additional stabilization due to the resistance of the soliton's inner structure to azimuthal modulations.

Above the instability border (in terms of Fig. 2), the growth of perturbations leads to the formation of a spot strongly confined in the azimuthal direction, see Fig. 3. One may expect that this spot will eventually suffer intrinsic collapse under the action of the cubic nonlinearity in the 2D space (in the presence of a periodic modulation of the refractive index, the onset of the collapse in 2D media may differ from that in free space, while the eventual asymptotic stage

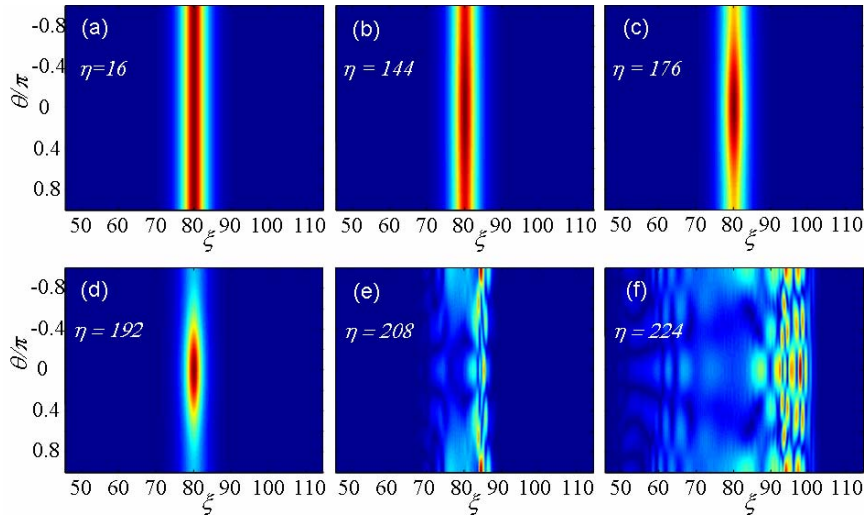

FIG. 3. (Color online) Evolution of the annular soliton above the instability threshold in the self-focusing medium. Here and in Figs. 4 and 5 below, parameters are $\xi_0=80$, $\sqrt{\alpha}/\xi_0=0.84$, and $Q=0.5$.

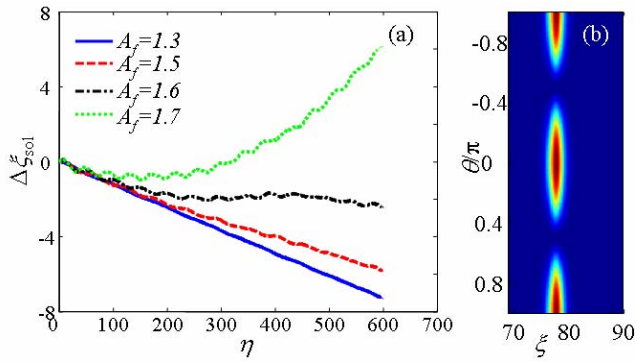

FIG. 4. (Color online) Dynamics of annular dipole solitons in the self-defocusing medium. (a) Shrinkage-expansion at different values of the amplitude of the modulating factor, $A_f \cos\theta$. (b) The intensity profile of a stable dipole soliton along the angular variable.

of the collapse development is essentially the same [20]). Due to limitations of our numerical scheme, the collapse actually stops in the simulations, and the field distribution breaks down. In the real physical medium, the collapse continues until causing damage to the material.

In the SDF medium ($\sigma=-1$), Eq. (9) predicts that all annular solitons are stable regardless of their amplitude and α. This prediction of the above analysis was verified by direct numerical integration of Eq. (4). In addition, the SDF medium supports new stable solutions featuring permanent modulation in the azimuthal direction. These solutions correspond to cnoidal-wave solutions of Eqs. (6) with $\sigma=-1$,

$$U=-V=e^{-i\omega\eta}k\sqrt{(\omega-1)/(1+k^2)}\,\mathrm{sn}[\sqrt{2(\omega-1)/(1+k^2)}y], \tag{11}$$

where sn is the elliptic sine with modulus k, and the frequency, $\omega>1$, is subject to the periodicity condition

$$\omega-1=2[nK(k)/\pi]^2(1+k^2)(\alpha/\xi_0{}^2), \quad n=1,2,\ldots \tag{12}$$

(K is the complete elliptic integral). Solutions (11) corresponding to $n=1$ and 2 in Eq. (12) resemble, respectively, the recently found stable dipole and quadrupole solutions of the 2D NLS equation which combines a radial Bessel-lattice potential and the self-defocusing cubic nonlinearity [21].

As concerns stability of the solutions given by Eq. (11), only the dipole-mode azimuthally modulated states, corresponding to $n=1$ in Eq. (12), are stable in the simulations, whereas the quadrupole and higher-order circular solitons are unstable in the present model with $\sigma=-1$. To illustrate the self-trapping of stable dipole solitons, Fig. 4(a) depicts the radial motion of the center of the annular soliton onto which a dipolar modulation was imposed, by multiplying it with factor $A_f \cos\theta$. If the modulation factor is taken with $A_f<1.6$, the dipole ring shrinks continuously, while for larger A_f it initially shrinks and then undergoes radial expansion, eventually leading to collapse. However, for A_f close to 1.6, the dipole soliton initially shrinks but then reaches a stable steady-state shape. Figure 4(b) depicts the steady-state intensity profile of the thus formed *stable* circular dipole soliton, for $A_f=1.6$.

As mentioned above, we have also studied the stability of the AGS modulated into higher-order azimuthal profiles, viz., quadrupoles and hexapoles. In these cases, initial conditions are generated by the multiplication of the annular soliton with higher-order modulating factors, $A_f \cos(2\theta)$ for the quadrupole, and $A_f \cos(3\theta)$ for the hexapole. Unlike the case of the circular dipole solitons, the quadrupole and hexapole azimuthal modulations always initiate continuous shrinkage of the ring, regardless of amplitude A_f. Figure 5 shows the evolution of the ring's radius for the quadrupole (a) and hexapole (b) modulations, with various values of A_f. It can be seen that, in contrast to the dipole case, the amplitude does not affect the shrinkage rate, and the shrinkage cannot be reversed. Actually, the hexapoles exhibit a faster shrinkage rate, approximately twice that of the quadruples. Attempts to reverse the shrinkage by a further increase of the amplitude resulted in complete disintegration of the solution.

Vortex rings, alias *whispering-gallery-mode patterns*, where studied too. They can be obtained from stable annular solitons, multiplying them by $A_f \exp(im\theta)$, with integer m. The thus generated states exhibit noteworthy behavior. For A_f below a certain threshold (which depends on vorticity m), the vortex ring shrinks at a constant rate. Above the threshold, it splits, in the radial direction, into two rings with oscillating amplitudes, one rapidly shrinking and the other rapidly expanding, see an example in Fig. 6. Both secondary rings retain the original topological charge of the excitation ($m=1$ in Fig. 6). Higher-order vortices, i.e., ones with $m>1$, demonstrate unstable evolution similar to that of the quadrupole and hexapole states. For smaller A_f, higher-order vortex rings continuously shrink, but faster than their coun-

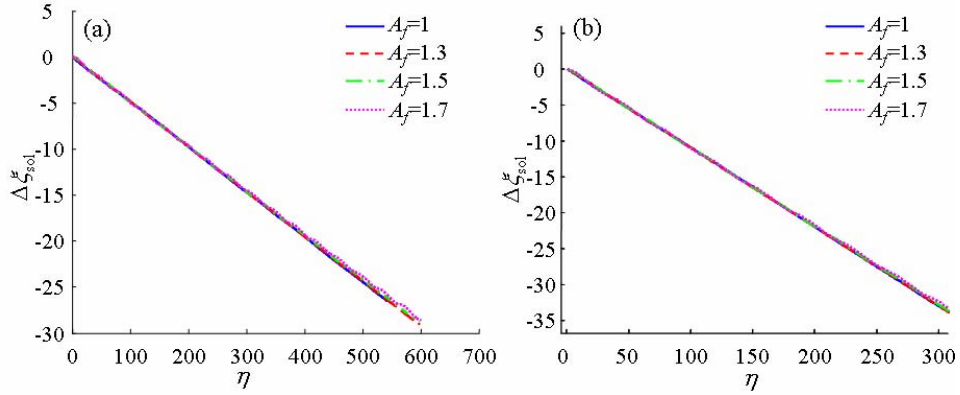

FIG. 5. (Color online) Evolution of the radius of circular solitons of the quadrupole (a) and hexapole (b) types in the self-defocusing medium (solitons of these types are always unstable, see text).

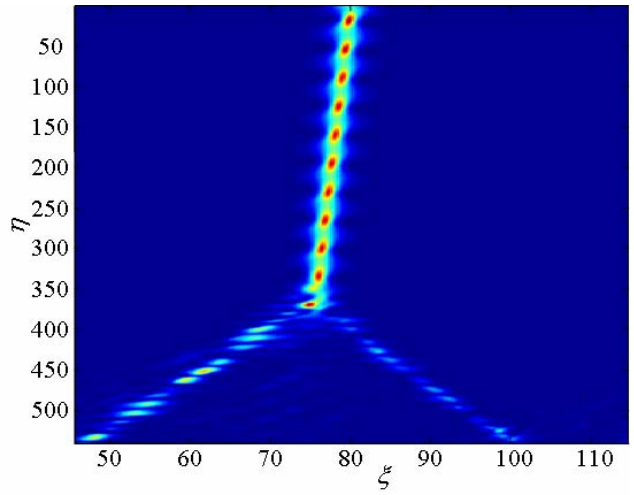

FIG. 6. (Color online) Splitting, in the radial direction, of the vortex ring with $m=1$, which was created by multiplying a stable annular soliton in the self-defocusing medium by $1.5\exp(i\theta)$.

terparts with $m=1$. Above a certain threshold, the vortex splits into two rings, similar to the scenario displayed in Fig. 6. It is relevant to mention that, in various 2D models of the NLS type, it has been found that the instability leads to splitting of vortex rings into sets of fragments in the azimuthal direction, see review [22], while the radial splitting was not reported before.

IV. DISCUSSION AND CONCLUSIONS

This work introduces families of standing annular gap solitons (AGSs), which represent "frozen light rings" in self-focusing (SF) and self-defocusing (SDF) Kerr media incorporating a chirped circular Bragg grating (CBG). In the SF case, an analytical approximation for the stability border of the annular solitons was derived and verified numerically. The SDF model supports unconditionally stable annular solitons, along with stable dipole solitons. Higher-order multipole solutions were found to be unstable in the SDF setting; they exhibit continuous shrinkage of the ring, with higher-order multipoles shrinking faster.

Vortex solitons in the SDF medium, alias whispering-gallery-modes states, which carry orbital angular momentum, were constructed too, and found to be unstable. In the course of the evolution, the vortex ring either continuously shrinks, or *splits* into two vortex rings in the radial direction, depending on the initial amplitude. In the latter case, one secondary ring shrinks rapidly, while the other one rapidly expands.

Lastly, it is relevant to mention a relation of the present model to another one, which includes a circular lattice and self-defocusing nonlinearity. It was recently introduced in Ref. [23] as the Gross-Pitaevskii equation for self-repulsive BEC trapped in a periodic radial potential:

$$i\psi_t = -(\psi_{rr} + r^{-1}\psi_r + r^{-2}\psi_{\theta\theta}) - \varepsilon\cos(2r)\psi + |\psi|^2\psi. \tag{13}$$

It is straightforward to demonstrate that coupled-mode equations (4) can be derived from Eq. (13) by means of substitution (2), for wave functions with the chemical potential taking values close to edges of *radial band gaps* in the linear spectrum of Eq. (13). It should be noted, however, that the radial-lattice potential in Eq. (13) is *periodic* in r, unlike the lattice profile introduced in Ref. [15] and used in the present work, which is *chirped*, as per the phase profile of the Hankel functions, that determine the shape of the lattice. In Ref. [23], it was demonstrated that Eq. (13) gives rise to families of stable ring-shaped radial gap solitons. It was also found that the ring solitons may carry stable pairs of azimuthal dark solitons, which are analogs of the dipole solitons found in the present work.

[1] Y. S. Kivshar and G. P. Agrawal, *Optical Solitons: From Fibers to Photonic Crystals* (Academic, San Diego, 2003); B. A. Malomed, *Soliton Management in Periodic Systems* (Springer, New York, 2006).

[2] J. Meier, G. I. Stegeman, Y. Silberberg, R. Morandotti, and J. S. Aitchison, Phys. Rev. Lett. **93**, 093903 (2004); Y. Linzon, Y. Sivan, B. Malomed, M. Zaezjev, R. Morandotti, and S. Bar-Ad, *ibid.* **97**, 193901 (2006).

[3] A. Trombettoni and A. Smerzi, Phys. Rev. Lett. **86**, 2353 (2001); P. J. Y. Louis, E. A. Ostrovskaya, C. M. Savage, and Y. S. Kivshar, Phys. Rev. A **67**, 013602 (2003); N. K. Efremidis and D. N. Christodoulides, *ibid.* **67**, 063608 (2003); K. E. Strecker, G. B. Partridge, A. G. Truscott, and R. G. Hulet, New J. Phys. **5**, 73 (2003); O. Morsch and M. Oberthaler, Rev. Mod. Phys. **78**, 179 (2006).

[4] D. N. Christodoulides and R. I. Joseph, Opt. Lett. **13**, 794 (1988).

[5] H. S. Eisenberg, Y. Silberberg, R. Morandotti, A. R. Boyd, and J. S. Aitchison, Phys. Rev. Lett. **81**, 3383 (1998).

[6] J. W. Fleischer, M. Segev, N. K. Efremidis, and D. N. Christodoulides, Nature (London) **422**, 6928 (2003).

[7] B. A. Malomed and P. G. Kevrekidis, Phys. Rev. E **64**, 026601 (2001).

[8] D. N. Neshev, T. J. Alexander, E. A. Ostrovskaya, Y. S. Kivshar, H. Martin, I. Makasyuk, and Z. Chen, Phys. Rev. Lett. **92**, 123903 (2004); J. W. Fleischer, G. Bartal, O. Cohen, O. Manela, M. Segev, J. Hudock, and D. N. Christodoulides, *ibid.* **92**, 123904 (2004); G. Bartal, O. Manela, O. Cohen, J. W. Fleischer, and M. Segev, *ibid.* **95**, 053904 (2005).

[9] J. Yang, I. Makasyuk, P. G. Kevrekidis, H. Martin, B. A. Malomed, D. J. Frantzeskakis, and Zhigang Chen, Phys. Rev. Lett. **94**, 113902 (2005).

[10] J. Scheuer and M. Orenstein, Science **285**, 230 (1999); Y. Yadin, J. Scheuer, Y. Gross, and M. Orenstein, Opt. Lett. **27**, 1908 (2002); J. Scheuer, Y. Yadin, Y. Gross, and M. Orenstein, *NLGW 99'* (Optical Society of America, Washington, D.C., 1999), WD30, p. 145.

[11] Y. V. Kartashov, A. A. Egorov, Victor A. Vysloukh, and L.

Torner, Phys. Rev. E **70**, 065602(R) (2004); J. Yang, New J. Phys. **6**, 47 (2004); Y. V. Kartashov, V. A. Vysloukh, and L. Torner, Phys. Rev. Lett. **93**, 093904 (2004); **94**, 043902 (2005); Q. E. Hoq, P. G. Kevrekidis, D. J. Frantzeskakis, and B. A. Malomed, Phys. Lett. A **341**, 145 (2005).

[12] X. S. Wang, Z. G. Chen, and P. G. Kevrekidis, Phys. Rev. Lett. **96**, 083904 (2006).

[13] T. Schwartz, G. Bartal, S. Fishman, and M. Segev, Nature (London) **446**, 52 (2007).

[14] J. Scheuer and A. Yariv, IEEE J. Quantum Electron. **39**, 1555 (2003); Phys. Rev. E **70**, 036603 (2004); J. Scheuer, W. M. J. Green, G. A. DeRose, and A. Yariv, Appl. Phys. Lett. **86**, 251101 (2005).

[15] E. Lidorikis, M. Soljačić, M. Ibanescu, Y. Fink, and J. D. Joannopoulos, Opt. Lett. **29**, 851 (2004).

[16] B. J. Eggleton, R. E. Slusher, C. M. de Sterke, P. A. Krug, and J. E. Sipe, Phys. Rev. Lett. **76**, 1627 (1996); B. J. Eggleton, C. M. De Sterke, and R. E. Slusher, J. Opt. Soc. Am. B **16**, 587 (1999).

[17] A. B. Aceves and S. Wabnitz, Opt. Lett. **17**, 1566 (1989); D. N. Christodoulides and R. I. Joseph, Phys. Rev. Lett. **62**, 1746 (1989).

[18] B. A. Malomed and R. S. Tasgal, Phys. Rev. E **49**, 5787 (1994); I. V. Barashenkov, D. E. Pelinovsky, and E. V. Zemlyanaya, Phys. Rev. Lett. **80**, 5117 (1998); A. De Rossi, C. Conti, and S. Trillo, *ibid.* **81**, 85 (1998).

[19] N. M. Litchinitser, B. J. Eggleton, and D. B. Patterson, J. Lightwave Technol. **15**, 1303 (1997); N. M. Litchinitser, B. J. Eggleton, C. M. de Sterke, A. B. Aceves, and G. P. Agrawal, J. Opt. Soc. Am. B **16**, 18 (1999).

[20] B. B. Baizakov, B. A. Malomed, and M. Salerno, Europhys. Lett. **63**, 642 (2003); Phys. Rev. A **70**, 053613 (2004).

[21] Y. V. Kartashov, R. Carretero-Gonzalez, B. A. Malomed, V. A. Vysloukh, and L. Torner, Opt. Express **13**, 10703 (2005).

[22] B. A. Malomed, D. Mihalache, F. Wise, and L. Torner, J. Opt. B: Quantum Semiclassical Opt. **7**, R53 (2005).

[23] B. B. Baizakov, B. A. Malomed, and M. Salerno, Phys. Rev. E **74**, 066615 (2006).